

PAPER • OPEN ACCESS

Passivation Mechanisms of Atomic Layer-deposited AlO_x Films and $\text{AlO}_x/\text{SiO}_x$ Stack

To cite this article: Lei Gong *et al* 2019 *IOP Conf. Ser.: Mater. Sci. Eng.* **585** 012026

View the [article online](#) for updates and enhancements.



IOP | ebooks™

Bringing you innovative digital publishing with leading voices to create your essential collection of books in STEM research.

Start exploring the collection - download the first chapter of every title for free.

Passivation Mechanisms of Atomic Layer-deposited AlO_x Films and $\text{AlO}_x/\text{SiO}_x$ Stack

Lei Gong^{1,2}, Chunlan Zhou^{1,2,*}, Junjie Zhu³, Wenjing Wang^{1,2}, Fangxu Ji^{1,2}

¹The Key Laboratory of Solar Thermal Energy and Photovoltaic System, Institute of Electrical Engineering, Chinese Academy of Science (CAS), Beijing 100190, PR China

²University of Chinese Academy of Sciences (UCAS), Beijing 100190, PR China

³Solar Energy Department, Institute for Energy Technology, Kjeller, Norway

*E-mail: zhouchl@mail.iee.ac.cn

Abstract. A new passivation layer of $\text{AlO}_x/\text{SiO}_x$ were prepared, in which 80 nm SiO_x was prepared by spin-coating perhydropolysilazane (PHPS) and annealed at 450 °C. In order to compare the passivation effect of single AlO_x layers and the $\text{SiO}_x/\text{AlO}_x$ stack on silicon surface, the fixed charge (Q_f) in the passivated layers and chemical passivation effect were obtained by corona charge method. Fourier transform infrared spectroscopy (FTIR) and Time-of-flight secondary ion mass spectrometry (TOF-SIMS) was used to investigate the Si-H, Si-O bonds and the hydrogen profile in the passivation layer, respectively. The result reveals that the single layer of AlO_x provides good field effect with a large amount of negative Q_f . Furthermore, SiO_x capping on AlO_x have more excellent chemical passivation because of amount of H saturate the dangling bonds on the silicon surface.

1. Introduction

Dangling bonds are formed on the surface of the silicon due to the broken of periodicity, causing a large increase in carriers surface recombination velocity [1]. Surface passivation technology can effectively reduce the of carriers surface recombination velocity and increase effective minority carrier lifetime τ_{eff} of silicon by chemical passivation and field-effect passivation [2, 3]. Chemical passivation reduces the interface state density (D_{it}). For example, H and O atoms can saturate the dangling bonds at the silicon surface; the field effect passivation forms electric field which electrostatically shields the charge carriers from the interface, so the carrier surface recombination velocity can be reduced because of the lower possibility of meeting for the two type of carriers. A decreased surface recombination velocity means higher carrier lifetimes and thus higher efficiency cells. Different passivation materials have different fixed charge polarities. Among the commonly used passivation materials, AlO_x has negative fixed charges [4], while SiO_x and SiN_x have positive fixed charges [5]. AlO_x have attracted considerable attention due to their excellent surface passivation properties, surface recombination velocities below 10 cm/s have been demonstrated for several deposition methods of AlO_x layers such as atomic layer deposition (ALD), plasma-enhanced chemical vapor deposition (PECVD), and atmospheric pressure chemical vapor deposition (APCVD) [6-9]. However, in order to improve the firing stability, the Al_2O_3 layer usually is capped with a PECVD silicon nitride (SiN_x) layer [10]. In this work, we used PHPS to fabricate SiO_x capping layer on the ALD AlO_x passivation layers to improve the passivation on silicon surface, and compare the passivation quality of ALD AlO_x and $\text{AlO}_x/\text{SiO}_x$ stacks and their passivation mechanism.



2. Experiments

In the experiment, an N-type double-sided polished c-Si substrate was adopted with resistivity of 1~10 $\Omega\cdot\text{cm}$. After immersing in $\text{H}_2\text{SO}_4:\text{H}_2\text{O}_2=4:1$ (volume ratio) for 10 minutes at 85 $^\circ\text{C}$ and rinsing in DI water, 1% HF was used to remove the surface oxide layer. The AlO_x layer with different thicknesses of 5-20 nm was prepared by ALD on both sides of the substrate and was annealed in an air atmosphere at 400 $^\circ\text{C}$ for 10 min. The mixed solution of PHPS: n-butyl ether = 1:2 (volume ratio) was spun-coating on the double-side AlO_x surface at 4500 r/min for 60 s and then the coating was baked at 150 $^\circ\text{C}$ for 3 min. Finally, the $\text{AlO}_x/\text{SiO}_x$ stack is annealed in air atmosphere at 450 $^\circ\text{C}$ for 15 min. To exclude the effect of annealing step after deposition of SiO_x layers on AlO_x , we compare the passivation effect of AlO_x annealing at 400 $^\circ\text{C}$ for 10 min and two-step annealing which is annealing at 400 $^\circ\text{C}$ for 10 min and then at 450 $^\circ\text{C}$ for 15 min in an air atmosphere, the results show there is little different in the τ_{eff} . So a single AlO_x was just annealed in an air atmosphere at 400 $^\circ\text{C}$ for 10 min as a reference.

Ellipsometer was used to obtain the thickness of AlO_x and SiO_x layers. In this paper, the SiO_x layer thickness is identical at 80 nm. The lifetime samples were characterized using the Microwave Photoconductive Decay (μ -PCD, WT 2000, Semilab) method and the interface fixed charge was measured by the corona charge method using the same device. The chemical bond of the sample was characterized by FTIR, and the profile of H^+ and SiH^+ in passivation layers was tested by TOF-SIMS.

3. Results and Discussions

For samples with different AlO_x thicknesses, we measured the τ_{eff} , Q_f and minimum minority lifetime (τ_{min}) by corona charge method to evaluate the total passivation effect, field-effect passivation effect and chemical passivation effect of the film. Figure 1 shows the function of τ_{eff} with the corona charge for silicon passivated by single AlO_x film and the $\text{AlO}_x/\text{SiO}_x$ stack. By continuously applying charges opposite to Q_f to the surface of the sample, the electric field provided by the additional charge is used to offset the effect of field effect passivation, and the τ_{eff} continues to decrease. As the additional charge increases further until the field effect passivation is completely cancelled, τ_{eff} reaches a lowest value τ_{min} . The amount of charge applied at this point is regarded as the amount of Q_f of the interface. The τ_{min} has a strong positive relationship with the chemistry passivation effect, namely the reverse relationship with D_{it} . The corona charge decreases to 200 from 250 nC/cm^2 and τ_{min} is up to 400 from 300 μs after capping SiO_x layer on AlO_x . This means that the Q_f amount declines slightly while D_{it} has been evidently reduced. As the charge continues to be applied, the excess charge will again provide the effect of field effect passivation, so there will be a corresponding increase in τ_{eff} . The τ_{eff} and τ_{min} of the single layer of AlO_x and $\text{AlO}_x/\text{SiO}_x$ stacks of different AlO_x thicknesses are shown in Fig. 2. As the thickness of AlO_x increases from 5 nm to 20 nm, the τ_{eff} of both structures is gradually increasing, and the increasing trend is gradually slowing down. In addition, we measured that τ_{eff} of the single-layer SiO_x is about 350 μs . Comparing with the single-layer SiO_x and AlO_x , the τ_{eff} of the stack is higher than that of the single passivation layer, which means the passivation effect of the stack is better. The thickness of AlO_x shows little effect on Q_f of the two structures, the fixed charge of all single-layer AlO_x samples is maintained at $-1.6 \times 10^{12}/\text{cm}^2$, while the fixed charge of the $\text{AlO}_x/\text{SiO}_x$ stack is $-1.3 \times 10^{12}/\text{cm}^2$. This means that the SiO_x cap will slightly weaken the field passivation while increasing the chemical passivation. It also indicates regardless of in the single AlO_x or in the stack, that the main reason for the improvement of the passivation effect as the thickness of AlO_x increases is the enhancement of chemical passivation.

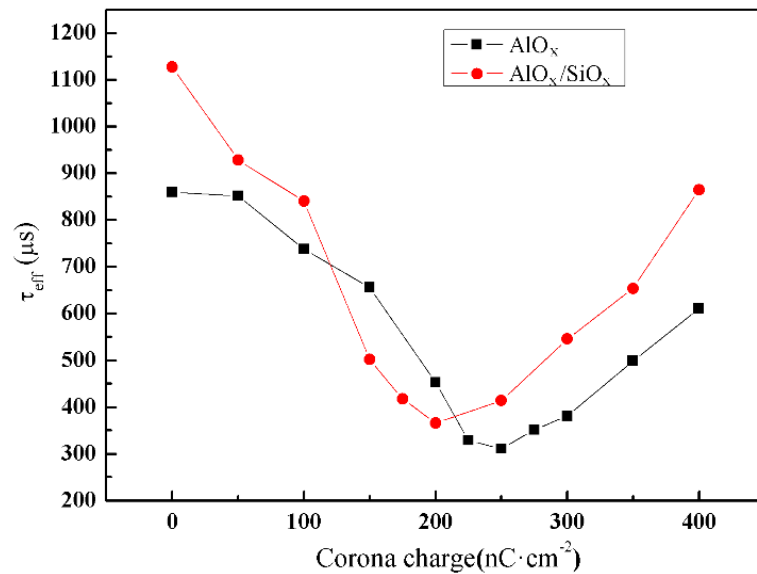


Figure 1. The corona charge curve of 15 nm AlO_x and the AlO_x/SiO_x stack. The corona charge and τ_{eff} at the lowest point represents the field-effect passivation and the chemical passivation, respectively

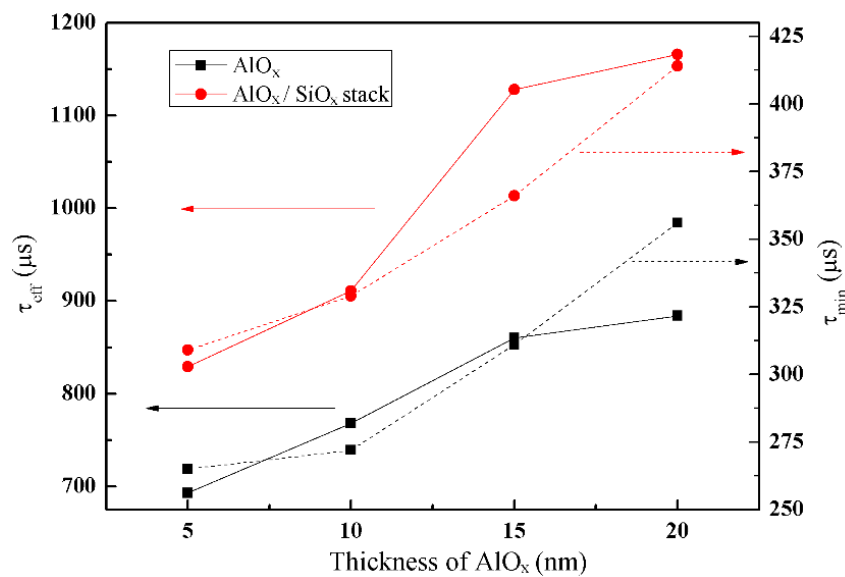


Figure 2. τ_{eff} and τ_{min} of single layer of AlO_x and the AlO_x/SiO_x stack varies with the thickness of AlO_x layer. The AlO_x layer was annealed in atmosphere at 400 °C for 10 min. After that, SiO_x was prepared and the stack was annealed in atmosphere at 450 °C for 15 min

In order to investigate the difference in the chemical passivation effect of these three structures, FTIR was measured and the results are shown in Fig. 3(a). After thermal treatment, PHPS has basically been converted into SiO_x, a small amount of Si-N is remained but it is negligible compared with Si-O. The Si-H peak at 2200 cm⁻¹ of AlO_x and the AlO_x/SiO_x stack plays a major role on chemical passivation. The absence of Si-H bonds in the single-layer SiO_x film illustrates the limited passivation effect is (τ_{eff} = 350 μs) because of the poor chemical passivation. Figure 3(b) presents the results of TOF-SIMS for the stack. It shows that the concentration of H⁺ is at a high level in both SiO_x layer and AlO_x layer. We can find an obvious peak of SiH⁺ near the surface of the Si substrate, which means an amount of H combined with Si to form Si-H and saturate the dangling bonds on the silicon surface. The result of FTIR indicates that there is no Si-H peak in the single layer of SiO_x. However,

SiH^+ in the SiO_x layer of the $\text{AlO}_x/\text{SiO}_x$ stack is obvious. This may due to H in the AlO_x which diffuses into the layer and is stored in it by combining with Si atoms.

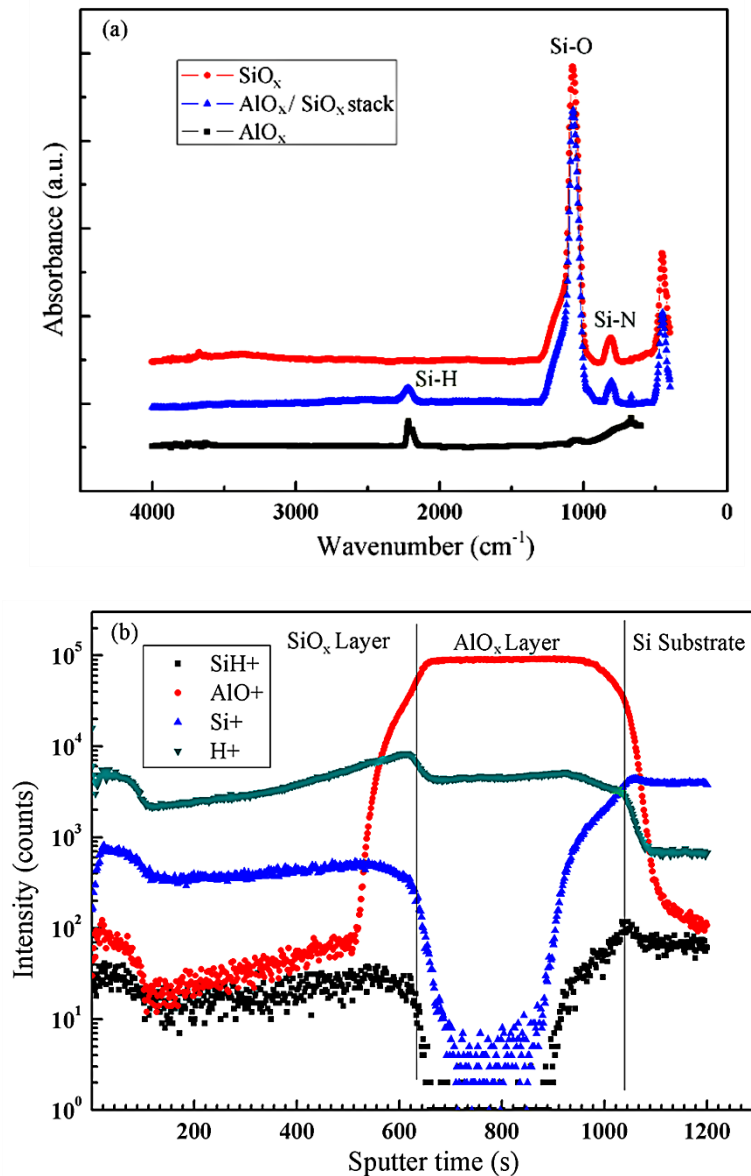


Figure 3. FTIR and the TOF-SIMS results. (a) is the FTIR spectrum of SiO_x layer, $\text{AlO}_x/\text{SiO}_x$ stack and AlO_x layer; (b) is the TOF-SIMS spectrum of $\text{AlO}_x/\text{SiO}_x$ stack. The position of each layer is marked in the figure. The sputter area is a square of $5 \mu\text{m} * 5 \mu\text{m}$.

4. Conclusions

In this paper, we present a new stack passivation layers of ALD $\text{AlO}_x/\text{SiO}_x$, in which 80 nm SiO_x was prepared by coating a PHPS precursor and annealed at 450°C in air atmosphere. If using single SiO_x layer to passivate the Si surface, the τ_{eff} is about $340 \mu\text{s}$ because it just provides the field-effect passivation. However, as for the single layer of AlO_x , τ_{eff} increases from $700 \mu\text{s}$ to $890 \mu\text{s}$ while thickness of AlO_x increasing from 5 nm to 20 nm. The negative fixed charge keeps constant but the chemical passivation increase with the increase of AlO_x thickness. After capping on AlO_x with SiO_x , the surface passivation of Si improves further, and τ_{eff} is in the range of 820-1150 μs as AlO_x thickness varies from 5 nm to 20 nm. Even though Q_f decreases from $-1.6 \times 10^{12}/\text{cm}^2$ to $-1.3 \times 10^{12}/\text{cm}^2$ after

capping SiO_x layers, the amount of H saturate the dangling bonds on the silicon surface still improves the surface passivation of Si.

5. Acknowledgments

The financial support from the research project 61874120 supported by National Natural Science Foundation of China and the research project 261574 granted by Norwegian Research Council are gratefully acknowledged.

6. References

- [1] Cartier E, Stathis J H and Buchanan D A, Passivation and depassivation of silicon dangling bonds at the Si/SiO₂ interface by atomic hydrogen, *Appl. Phys. Lett.* **63** (11) (1993) 1510-12
- [2] Glunz S W, Biro D, Rein S and Warta W, Field-effect passivation of the SiO₂/Si interface, *J. Appl. Phys.* **86** (1) (1999) 683-91
- [3] Sieber N, Mantel B F, Seyller T, Ristein J and Ley L, Electronic and chemical passivation of hexagonal 6H-SiC surfaces by hydrogen termination, *Appl. Phys. Lett.* **78** (9) (2001) 1216-18
- [4] Dingemans G, Terlinden N M, Verheijen M A and Kessels W M, Controlling the fixed charge and passivation properties of Si(100)/Al₂O₃ interfaces using ultrathin SiO₂ interlayers synthesized by atomic layer deposition, *J. Appl. Phys.* **110**(9) (2011) 042112
- [5] Töfflinger J A, Laades A, Leendertz C, Montañez L M, Korte L, Rech B and Stürzebecher U, PECVD-AlO_x/SiN_x Passivation Stacks on Silicon: Effective Charge Dynamics and Interface Defect State Spectroscopy, *Energy Procedia.* **55** (2014) 845-54
- [6] Werner F, Stals W, Görtzen R, Veith B, Brendel R and Schmidt J, High-rate atomic layer deposition of Al₂O₃ for the surface passivation of Si solar cells, *Energy Procedia.* **8** (4) (2011) 301-6
- [7] Black L E, Allen T, McIntosh K R and Cuévas A, Improved Silicon Surface Passivation of APCVD Al₂O₃ by Rapid Thermal Annealing, *Energy Procedia* **92** (2016) 317-25
- [8] Hoex B, Heil S B, Langereis E, Sanden and Kessels W M, Ultralow surface recombination of c-Si substrates passivated by plasma-assisted atomic layer deposited Al₂O₃, *Appl. Phys. Lett.* **89** (4) (2006) 271
- [9] Dingemans G, Mcm S V and Kessels W, Plasma-enhanced Chemical Vapor Deposition of Aluminum Oxide Using Ultrashort Precursor Injection Pulses, *Plasma Processes Polym.* **9** (8) (2012) 761-71.
- [10] Schmidt J, Veith B and Brendel R, Effective surface passivation of crystalline silicon using ultrathin Al₂O₃ films and Al₂O₃/SiN_x stacks, *Phys. Status Solidi RRL.* **3**(9) (2010) 287-9